Microbial Pathogenesis 105 (2017) 346–355

Contents lists available at ScienceDirect

Microbial Pathogenesis

journal homepage: www.elsevier.com/locate/micpath

Tailoring shape and size of biogenic silver nanoparticles to enhance antimicrobial efficacy against MDR bacteria

Madhuree Kumari, Shipra Pandey, Ved Prakash Giri, Arpita Bhattacharya, Richa Shukla, Aradhana Mishra*, C.S. Nautiyal

CSIR-National Botanical Research Institute, Rana Pratap Marg, Lucknow, 226 001, India

ARTICLE INFO

Article history:
Received 15 March 2016
Received in revised form
17 October 2016
Accepted 21 November 2016
Available online 23 November 2016

Keywords:
Silver nanoparticles
Trichoderma viride
Shape and size
Antimicrobial activity
Synergistic effect
Antibiotics

ABSTRACT

Spherical, rectangular, penta, and hexagonal silver nanoparticles of different dimensions were biosynthesized in an eco-friendly manner by biocontrol agent, *Trichoderma viride* by manipulating physical parameters, pH, temperature, and reaction time. The particles were characterized by UV–vis spectroscopy; Dynamic Light Scattering (DLS), Transmission Electron Microscopy (TEM) and Fourier Transform Infra-red Spectroscopy (FTIR). Shape and size dependent antimicrobial activity of nanoparticles against human pathogens was observed. Maximum inhibition was found with spherical nanoparticles (2–5 nm) showing 40, 51, 43, 53.9 and 55.8% against *Shigella sonnei*, *Escherichia coli*, *Serratia marcescens*, *Staphylococcus. aureus* and *Pseudomonas aeruginosa* respectively, where as pentagonal and hexagonal nanoparticles (50–100 nm) demonstrated 32, 41, 31, 42.84 and 42.80% of inhibition as compared to control. Nanoparticles of different geometry and dimension established enhanced antagonistic activity against pathogens with all the tested antibiotics. Excellent antimicrobial efficacy was obtained with spherical nanoparticles of 2–5 nm with ampicillin and penicillin. Shape and size played major role in enhancing antimicrobial potential of silver nanoparticles, both singly and synergistically with antibiotics which can be exploited to combat the spread of multidrug resistant pathogens.

1. Introduction

In the era of nanotechnology, silver nanoparticles are leading towards obtaining the status of wonder drug, combating the problem of multiple drug resistance (MDR) acquired by several pathogenic microbes [1,2]. Being able to kill pathogens by multiple modes, including DNA unwinding, membrane disruption, changing permeability of membrane, and production of free radicals, makes it a suitable candidate for medical applications as a potential antimicrobial agent [3,4].

The key properties and biomedical application of silver nanoparticles heavily rely upon the shapes and size of silver nanostructures. Thus, it becomes very important to establish protocols for controlled synthesis of silver nanoparticles [5,6]. Pal et al. [6] and Dong et al. [7] reported the shape dependent antimicrobial properties of chemically synthesized silver nanoparticles against *Escherichia coli*. Similarly, size dependent antimicrobial effect of silver nanoparticles has been demonstrated by Agnihotri et al. [8]. Though, chemically it has been possible to manipulate the architecture of silver nanoparticles, still it remains a mammoth task, regulating shapes and size of silver nanoparticles by biological approach [9–11]. Chemical synthesis of multishaped silver nanoparticles can be achieved by reducing agents such as poly (*N*-vinyl pyrrolidone), poly acrylic acid and capping with several organic solvents which may arise several environmental concerns [12–15]. Biosynthesis of multishaped silver nanoparticles by a non-pathogenic *Trichoderma viride* provides a green and economical solution to the lacuna for tailoring shape and size of silver nanoparticles through biological means [16,17]. By simply manipulating growth parameters of *T. viride*, the best shapes and size of biogenic silver nanoparticles, having enhanced abilities to combat pathogens can be obtained. Changing the parameters such as pH, temperature, reaction time, concentration of substrate and cell free extract has the potential to influence the size and geometry of synthesized nanoparticles [17,18]. Reports describing the individual effect of ion and cell free extract concentration, pH, reaction time, and temperature on formation of different geometry and

* Corresponding author. Division of Plant Microbe Interactions, CSIR-National Botanical Research Institute, Rana Pratap Marg, Lucknow, 226001, India.
E-mail address: mishramyco@yahoo.com (A. Mishra).

http://dx.doi.org/10.1016/j.micpath.2016.11.012
0882-4010/

dimension of nanoparticles [19,20] are available, but the mutually dependent effects of biological and physical parameters affecting morphologies of biosynthesized silver nanocrystals has not been elucidated yet. Thus, it becomes very important to decipher the exclusive balance of different parameters to create the optimum reaction conditions where a monodispersed population of different shapes and size could be obtained.

Biogenic silver nanoparticles have shown synergistic effects with antibiotics which can resist the polydrug resistance acquired by several pathogenic microbes [2,21]. For instance, *E. coli* shows resistance to a variety of antibiotics like ampicillin, kanamycin, streptomycin, and ticarcillin but cannot escape the synergistic actions of silver nanoparticles and antibiotics [2]. Several combinations of antibiotics or multidrug therapy have also evolved as an alternative mechanism to control multidrug resistance, but they still are not able to completely inhibit the MDR. Multidrug therapies either in combination therapy or sequential therapy is only able to slow down the evolution of multidrug resistance [22,23]. Silver nanoparticles, on the other hand, with their multiple modes of inhibitory actions, do not allow pathogens to acquire resistant against them [3,4]. Though, the effect of various shapes and sizes of biosynthesized silver nanoparticles along with antibiotics on multidrug resistant microbes still needs to be explored. *Shigella sonnei*, *E. coli*, *Serratia marcescens*, *Pseudomonas aeruginosa* and *Staphylococcus aureus* are common human pathogens causing shigellosis, diarrhoea, opportunistic infections, surgical infections, skin and respiratory tract infection respectively. These pathogens have acquired resistance against multiple antibacterial drugs, posing a major threat in developing countries [2]. A cost effective formulation is urgently required to fight these MDR pathogens more effectively, especially in developing countries to obtain a better livelihood without hampering the budget of poor people.

In current study, silver nanoparticles of various shapes and sizes were synthesized by a biocontrol agent, *T. viride* (MTCC 5661), and antimicrobial potential of biosynthesized nanoparticles were assessed against pathogens *S. sonnei*, *E. coli*, *S. marcescens*, *P. aeruginosa* and *S. aureus* singly and synergistically with antibiotics. Though there are many reports describing the synergistic effect of silver nanoparticles and antibiotics, to the best of our knowledge, this is the first report showing the effect of modulating dimension and geometry of silver nanoparticles on their synergistic antimicrobial potential with antibiotics.

2. Experimental

2.1. Materials and methods

The silver nitrate salt (ACS reagent, 99%) was purchased from Sigma Aldrich, USA. All other reagents used were of analytical grade. Potato dextrose agar (PDA), potato dextrose broth (PDB), nutrient agar (NA), nutrient broth (NB), luria bertani (LB) agar, luria bertani (LB) broth and antibiotics were purchased from HiMedia, Mumbai, India. All the solutions were prepared in double distilled water.

2.2. Microorganisms and culture conditions

T. viride (MTCC 5661) was isolated from CSIR-NBRI garden campus, and deposited in Microbial Type Culture Collection (MTCC), Chandigarh, India [17]. The culture was grown on PDA medium at 28 °C for 4 days and maintained at 4 °C in refrigerator.

A total of five pathogenic microbes *S. sonnei*, *E. coli*, *S. marcescens*, *P. aeruginosa* (ATCC 15692) and *S. aureus* (ATCC 33591) were used in this study. Microbial strains of *S. sonnei*, *E. coli* and *S. marcescens* were isolated from waste water of Varthur, Karnataka, India. All the cultures except *E. coli* were maintained on nutrient agar and experiments were conducted on nutrient broth. Maintenance and experiments of *E. coli* were performed with LB agar and LB broth.

2.3. Fungal cell free extract preparation and synthesis of silver nanoparticles of different shape and size

To prepare cell free extract, culture was grown in 100 ml of PDB for 4 days at 28 °C at rotation of 80 rpm. After 4 days, the biomass obtained was filtered and washed with autoclaved MQ water thrice and suspended in 100 ml of sterile deionized water for 3 days. For synthesis of silver nanoparticles, aqueous silver nitrate solution at a final concentration of 1 mM was added to the reaction flasks containing filtered 10% cell-free filtrate and incubated at 28 °C on a rotary shaker (150 rpm). Flasks containing cell free extract without silver nitrate and aqueous solution of silver nitrate without cell free extract of *T. viride* served as controls.

The reaction was carried out at 20, 30 and 40 °C, and pH was varied from 5.0, 7.0, to 9.0 at different time intervals of 24, 48 and 72 h. All the variations (pH, time, and temperature) were performed simultaneously to assess the combinatorial effect of different parameters on genesis of a particular shape and size.

2.4. Characterization of silver nanoparticles

Preliminary characterization of silver nanoparticles was done through visual observation for change in colour of cell free extract, and further confirmed by UV–vis spectroscopy (Thermo specrtoscan UV 2700) for appearance of characteristic surface plasmon resonance band of silver nanoparticles [24]. To observe the hydrodynamic diameter, their monodisperse nature, and their stability; dynamic light scattering (DLS) size, polydispersity index (PDI) and zeta potential was recorded from Malvern, nanoseries zeta sizer. To find the exact shape and size of nanoparticles, transmission electron microscopy (TEM) (Technai1321 G2 Spirit TWIN, USA) was carried out. Samples were filtered through 0.45μ syringe millipore filters and sonicated for 2 min. A drop of solution was deposited on formvar-coated copper grids, and left overnight for drying. Bright field TEM studies were carried out at 80 KV.

Fourier transform infra-red spectroscopy (FTIR) was carried out following the protocols of Kumari et al., 2016 [18]. For determining the percent conversion of silver salt to silver nanoparticles, inductively coupled plasma mass spectrometry (ICP-MS) studies were carried out following the protocols of Singh et al. [25] with some modifications. Briefly, the biosynthesized silver nanoparticles were collected by centrifugation of the total extract at 20,290 g for 20 min and thoroughly washed with deionized and double distilled water to remove unreacted or loosely bound Ag+ ions. One mM silver nitrate added in double distilled water served as control. Samples were digested (10 ml) in 3 ml of HNO_3 at temperature 80 °C for 2 h. Digested sample were diluted and quantity was analysed Inductive coupled Plasma mass spectrometer (ICP-MS, Agilent 7500cx). For calibration, standard material was of silver was used (300 ppb, Agilent).

2.5. Growth kinetics/antimicrobial activity

Antibacterial efficacy of silver nanoparticles of three different shapes, spherical, penta/hexagonal, rectangular, and two different sizes (2–5 and 40–50 nm) were evaluated against human pathogens, viz. *S. sonnei*, *E. coli*, *S. marcescens*, *S. aureus and P. aeruginosa*. The antibacterial activity was assessed by disk diffusion and CFU methods [16] with some modifications. To study the antagonistic effects of silver nanoparticles on pathogens, 100 μl of overnight grown cultures were spread uniformly on nutrient agar plates. Pre

sterilized cotton of 1 cm^2 was placed on the centre of the plates and pipetted with 50 μl of desired silver nanoparticles and allowed to air dry. The plates were incubated at 28 °C (37 °C for *E. coli*) for 24 h, after which the zone of inhibition was observed.

For CFU studies, 100 ml of nutrient broth and Luria Bertani broth were mixed with 10% of biogenic silver nanoparticles of different dimensions. 1% overnight grown cultures of pathogenic bacteria were inoculated and their colony forming units were counted after 24 h of inoculation.

To determine the synergistic effect of silver nanoparticle and antibiotics, cotton was impregnated with both standard concentration of antibiotics (10 mcg for ampicillin, penicillin G and streptomycin, 30 mcg for kanamycin and tetracyclin), and 50 μl of silver nanoparticles of different dimensions. The impregnated discs were placed onto agar plates which were preinoculated with 100 μl of test pathogenic strain. After 24 h of incubation, zone of inhibition was measured and compared with control of antibiotic alone disks [2].

3. Results and discussion

The cell free extract of *T. viride* was able to synthesize silver nanoparticles as observed from colour change and UV–vis spectroscopy (Fig. S1 and 1). After 24 h of addition of silver nitrate, colour of cell free extract changed from pale yellow to brown indicating formation of silver nanoparticles at different reaction conditions (Fig. S1). Silver nanoparticles exhibit phenomenon of surface plasmon resonance depicting a sharp peak between 400 and 500 nm. UV–vis spectrum of nanoparticles showed a sharp peak at 419–422 nm after 24 h of incubation indicating synthesis of stabilized silver nanoparticles (Fig. 1). Time dependent increase in intensity of synthesized nanoparticles was observed which was similar to earlier observations taken by Munger et al. [26]. Zeta potential of the synthesized particles was recorded to be −20.4 mV (Fig. S2). Zeta potential of nanoparticles depends on a number of factors including pH, temperature, concentration and ionic strength [27]. The zeta potential of the particles indicated that the particles were stable which reflected further in the studies of transmission electron microscopy.

Further, ICP-MS studies revealed 71.8% of silver nitrate has been converted into the silver nanoparticles using the cell free extract of *T. viride* (Fig. 2A).

FTIR studies of cell free extract of *T. viride* and biosynthesized silver nanoparticles were carried out to know the functional groups involved in coating of nanoparticles (Fig. 2B). The cell free extract exhibited peaks at 2391, 1059 and 973 cm^{-1} (Fig. 2Ba) which corresponded to asymmetric stretch of carbonyl group, secondary cyclic alcohol and bending vibration in tertiary methyl group respectively. Peaks at 1664 cm^{-1} were observed in both cell free extract and biosynthesized silver nanoparticles indicating the role of secondary metabolites in efficient coating of nanoparticles (Fig. 2Ba,b). Peak at 1664 cm^{-1} denoted non conjugated C=C stretching of amides and asymmetrical stretching of carboxylic acid or carbonyl group respectively [28,29]. The results clearly indicated that the nanoparticles were coated with proteins and organic acids present in cell free extract of *T. viride*.

The cell free extract of *T. viride* was able to form nanoparticles at wide range of pH (5.0–9.0), temperature (20, 30 and 40 °C) after 24 h of incubation as evident from hydrodynamic diameter taken from zeta sizer (Fig. S3). It ranged from 30 to 150 nm as the parameters were varied, but all demonstrated the poly dispersity index (PDI) value below 0.3 indicating the monodisperse nature of particles formed (Fig. S3). Zeta size indicates the size of particles along with the thickness of capping agent [30].

Further, effect of each parameter with respect to other parameters was studied in detail.

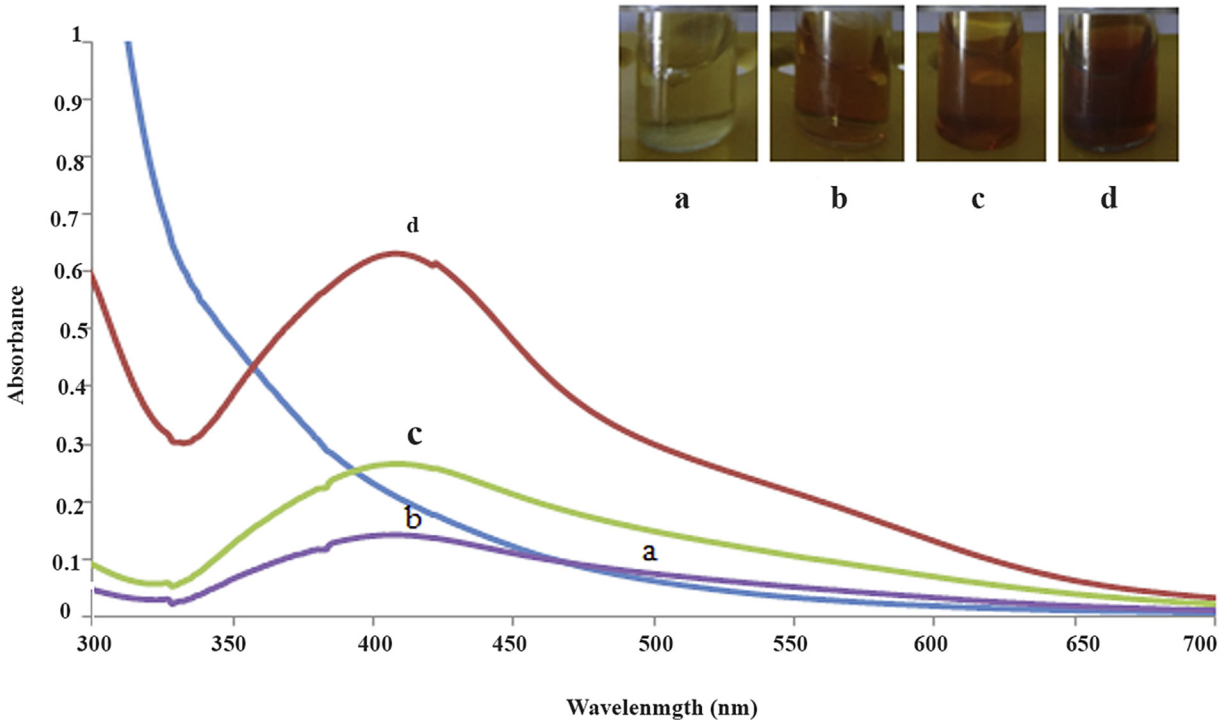

Fig. 1. UV–vis. spectra of silver nanoparticles biosynthesized by *T. viride* at different time intervals of (a) control (b) 24 h (c) 48 h (d) 72 h. Inset graph shows colour change in cell free extract with respect to time (a) control (b) 24 h (c) 48 h (d) 72 h due to formation of silver nanoparticles.

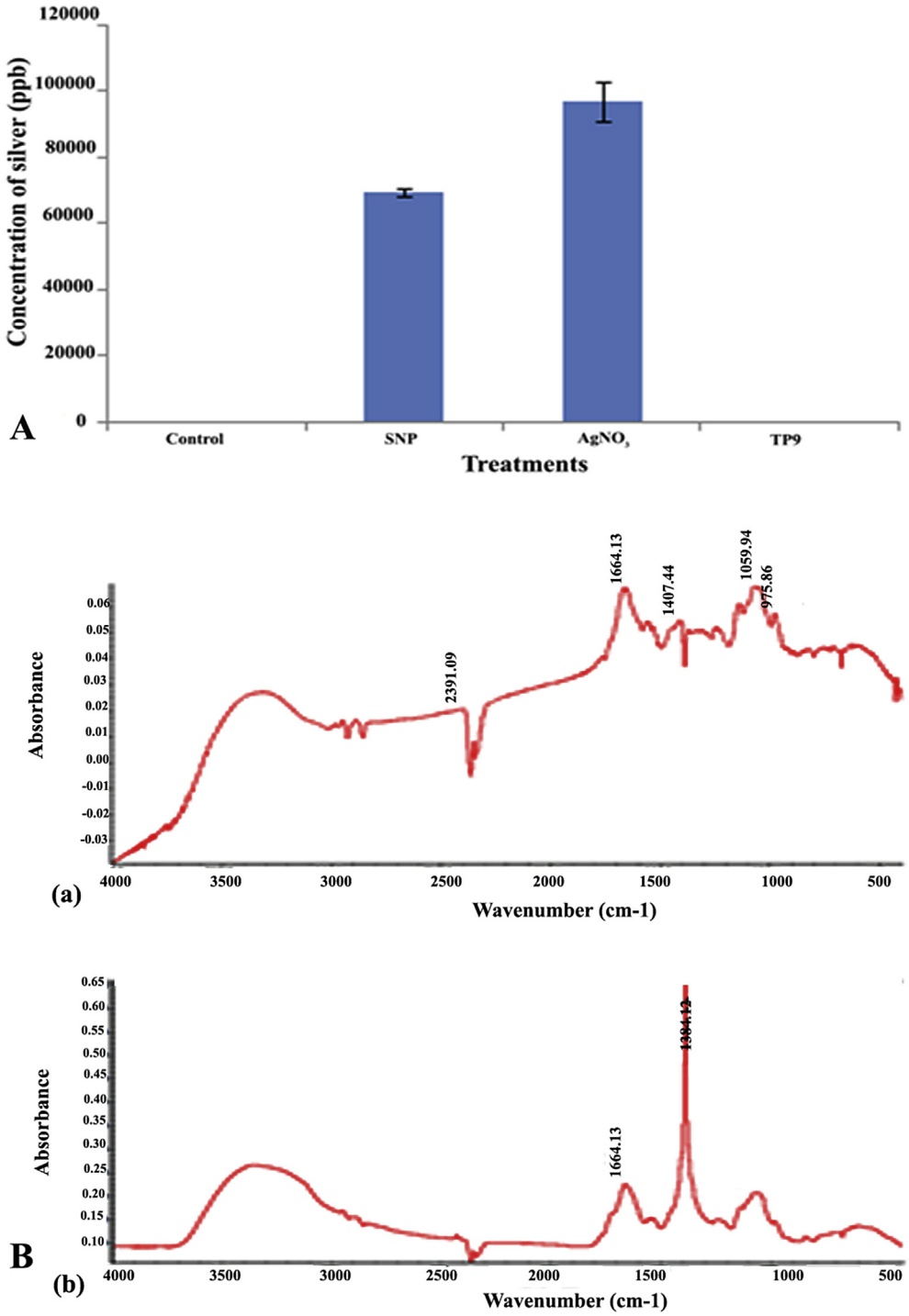

Fig. 2. (A) Reduction of silver nitrate into silver nanoparticles in presence of cell free extract of *T. viride* determined by ICP-MS (B) FTIR spectra of (a) cell free extract of *T. viride* (b) silver nanoparticles biosynthesized by cell free extract of *T. viride*.

3.1. Effect of different physical parameters on biosynthesis of silver nanoparticles

3.1.1. Effect of pH

Effect of three different pH 5.0, 7.0, and 9.0 at different temperature, and reaction time was observed for manipulation of silver nanoarchitecture. At pH 7.0, at different temperature and time, spherical nanoparticles below 50 nm were synthesized (Figs. 3–5), however at pH 5.0, and 9.0, the variation was observed at 40 °C after 72 h of incubation, where rectangular (40–65 nm) and penta/hexagons (50–100 nm) particles were synthesized (Fig. 3).

The activities of enzymes are highly dependent upon biological conditions such as pH, time and temperature [31] which can be manipulated to get different dimensions and geometry of nanoparticles. From the results, it was clear that temperature, time and pH played an interdependent role to modulate shape. Higher and lower pH (9.0 and 5.0) at elevated temperature (40 °C) might have triggered activation of different enzymes than normal physiological

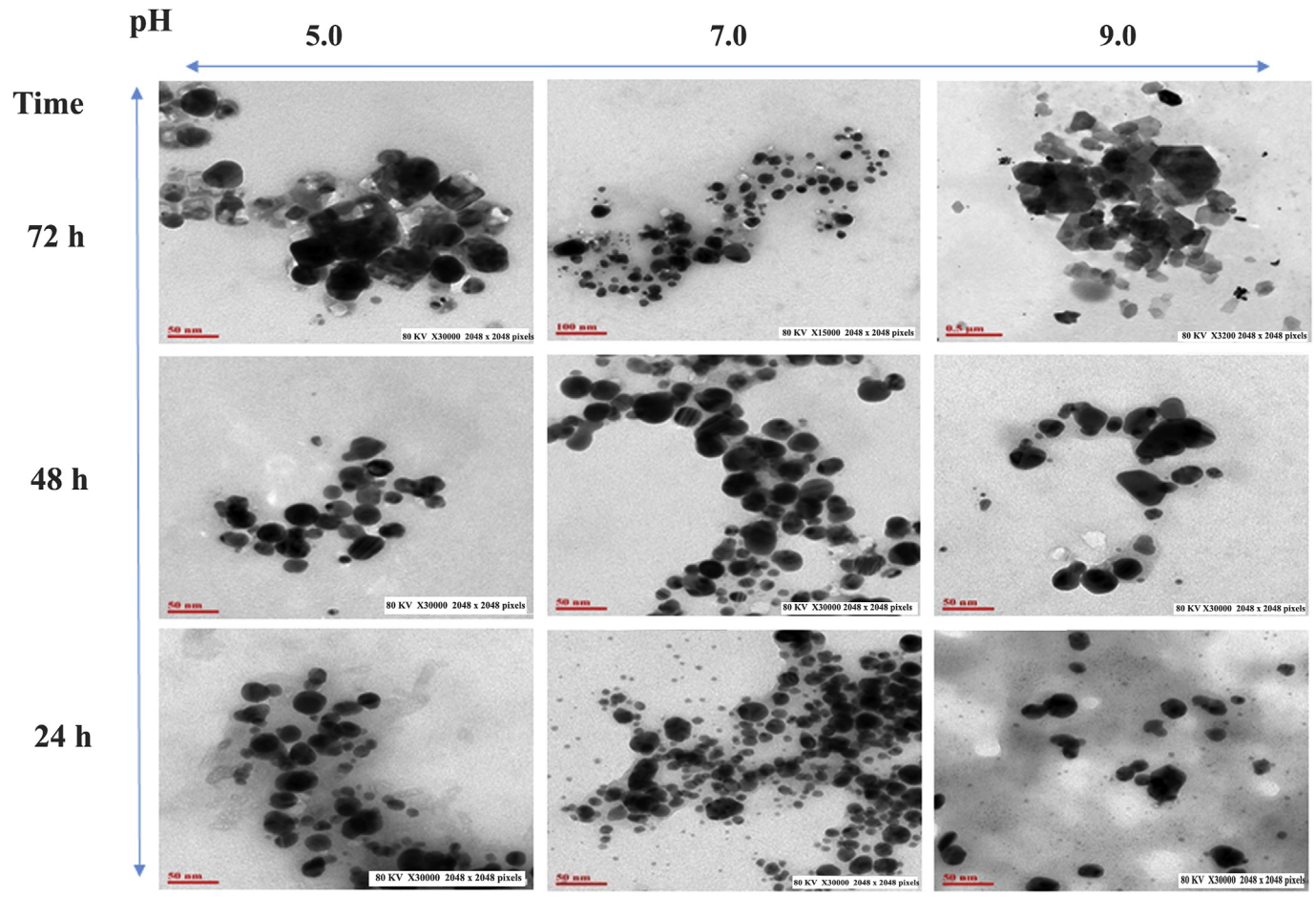

Fig. 3. Silver nanoparticles biosynthesized at 40 °C at pH 5.0, 7.0 & 9.0 at time intervals of 24, 48 and 72 h.

conditions resulting in a different direction of growth to the silver nuclei over the time period. Starnes et al. (2010) [31] has reported synthesis of rectangular gold nanoparticles at pH 9.0 *in planta*. Alteration in pH can cause change in oxidation and reduction state of functional moieties of enzymes [32], which along with time and temperature can produce novel morphologies of particles.

3.1.2. Effect of reaction time

Time played an important role in synthesis of spherical, penta/hexagonal, and rectangular nanoparticles along with pH and temperature (Figs. 3–5). Size of particles also increased from homogeneous population of 2–5 nm at 24 h (pH 7, 30 °C), to particles up to 80 nm after 72 h of incubation (Fig. 4). Same results were obtained at pH 5.0 at all different reaction conditions, however at pH 9.0, as the time interval increased from 24 to 72 h, the shape of silver nanoparticles also shifted from spherical to mixed consisting of spherical, triangular and rectangular particles at 40 °C. Growth of nanoparticles after formation of nuclei is strongly depended upon time [33]. It is well known that nanoparticle formation takes place in two stages (i) nucleation (ii) crystal growth [34]. After nucleation, where small spherical particles were formed, growth of nuclei caused the increase in size with respect to time.

Though successful attempts have been made to obtain different shapes and size of silver nanoparticles by chemical synthesis by varying reaction time and stirring time [35–37], still, there is research gap in area of biological manipulation for controlling shapes and size of silver nanoparticles.

3.1.3. Effect of temperature

Most prominent effect of temperature was observed at 40 °C where at pH 5.0 and 7.0, after 72 h of incubation, where penta/hexagonal and rectangular particles were synthesized (Fig. 3).

Different morphology was observed only at 40 °C, whereas the particles were not produced even at similar conditions when temperature was changed to 30 and 20 °C. Particles were mainly spherical and pseudospherical at 30 and 20 °C (Figs. 4 and 5). Increase in temperature increases the reaction rate, which along with different combination of physical parameters can yield different shapes and sizes of silver nanoparticles. Earlier, Song and Kim (2009) [16] and Jiang et al. [38] have also obtained different shapes of silver nanoparticles and enhanced rate of reaction by varying reaction temperature.

3.2. Mechanistic aspect for the synthesis of multishaped silver nanoparticles

As observed, one factor alone does not govern the transformation of silver seeds into different shapes and sizes; it is the unique balance and interdependent role of different physical parameters which lead to evolution of a particular morphology and dimension.

3.2.1. Spherical nanoparticles

Smallest spherical nanoparticles (2–5 nm) were obtained at 30 °C, pH 7.0 after 24 h of incubation. Every nanoparticle growth passes through two phases (i) nucleation (ii) crystal growth. In this

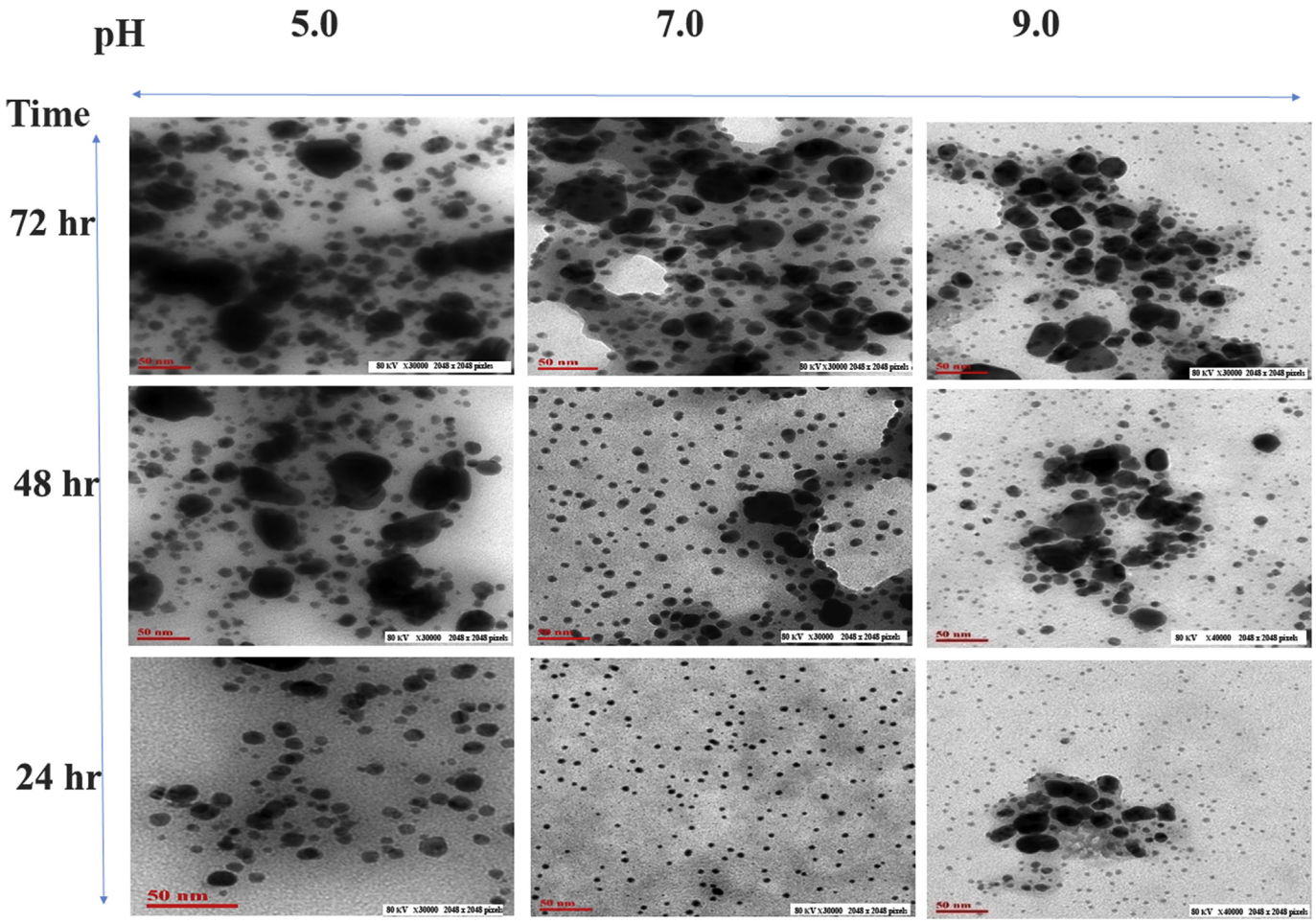

Fig. 4. Silver nanoparticles biosynthesized at 30 °C at pH 5.0, 7.0 & 9.0 at time intervals of 24, 48 and 72 h.

case, if particles were harvested early before entering the growth phase, their size remains smaller in form of spherical silver seeds (Fig. 6A). At 20 and 30 °C, the reaction rate was optimum, and as the time increased, growth of silver nuclei increased, resulting in larger particles, but of similar shape (Fig. 6B and C). Similar spherical gold nanoparticles were obtained by the same group by manipulating reaction rate and reaction time [18].

3.2.2. Rectangular nanoparticles

Rectangular nanoparticles of size 40–65 nm were synthesized at 40 °C, pH 5.0 after 72 h of incubation (Fig. 6D). The exact mechanism elucidating the conversion of silver seeds into different shapes still remains a challenging task. Different chemical methods have been proposed to obtain different shapes of silver nanoparticles [39,40], but the exact mechanism and function in biological system is yet to be explored. At 40 °C, rate of reaction is comparatively higher due to higher temperature, and due to effect of pH, selective adsorption of extract on different facets of silver seeds might have taken place resulting in genesis of rectangular nanoparticles.

3.2.3. Penta and hexagonal nanoparticles

Penta/hexagonal nanoparticles of size 50–100 nm were synthesized at 40 °C, pH 9.0 after 72 h of incubation (Fig. 6E). Similar to formation of rectangular particles, penta and hexagonal nanoparticles were also supposed to be synthesized due to unique balance of pH, temperature and time. Though sunlight-driven nanoprism and nanodecahedron were synthesized by Tang et al. (2015) [41], and different shapes were produced by *Taxus baccata* [42], but the mechanism has not been elucidated. This kind of shape might have resulted due to growth of anisotropic silver seeds and preferential binding of cell free extract at higher pH and high reaction rate. Xia et al. (2012) [43] have also demonstrated the selective binding of PVP and citrate on Ag(111) and Ag(100) surfaces, respectively, and thus favouring the formation of Ag nanocrystals enclosed preferentially by {111} or {100} facets resulting in cuboctahedrons, octahedrons, bare and plates.

3.3. Shape and size dependent antimicrobial activity of biosynthesized silver nanoparticles

Antimicrobial potential of three different shapes and two different spherical silver nanoparticles (2–5 and 40–50 nm), were evaluated against human pathogens, *S. sonnei*, *E. coli*, *S. marcescens*, *S aureus* and *P. aeruginosa* singly and in combination of different antibiotics.

Among the different shapes and sizes of nanoparticles, smallest spherical nanoparticles (2–5 nm) showed maximum zone of inhibition, followed by pentagonal and hexagonal nanoparticles (Fig. S4). Spherical nanoparticles of 2–5 nm formed zone of inhibition of 21.9, 23.6, 13.7, 23 and 23 mm for *S. sonnei*, *E. coli*, *S. marcescens*, *S. aureus* and *P. aeruginosa* respectively while with penta/hexagonal nanoparticle, zone of inhibition was 19.95, 21.2, 8.2, 21.75 and 21.5 mm for *S. sonnei*, *E. coli*, *S. marcescens*, *S. aureus*

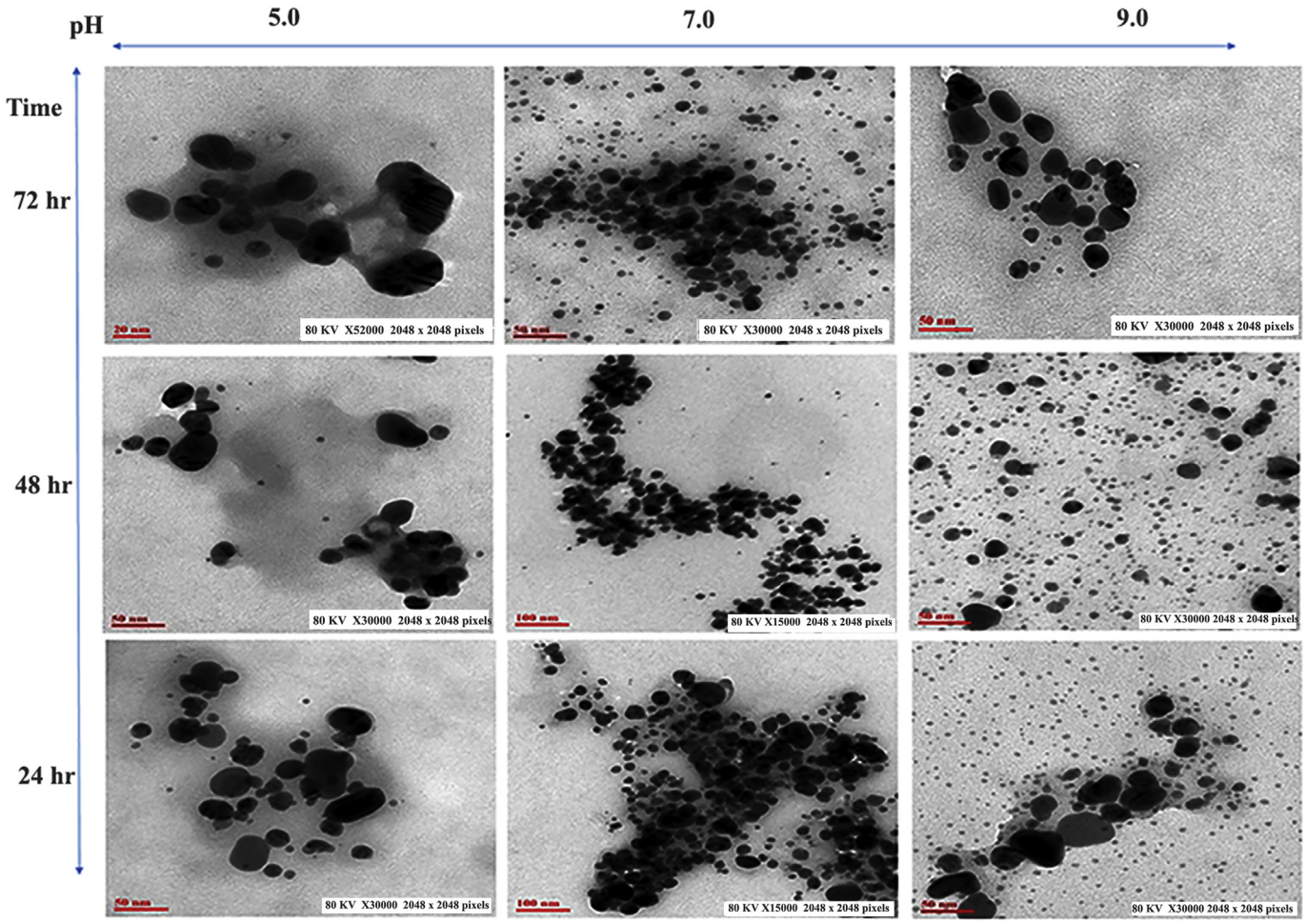

Fig. 5. Silver nanoparticles biosynthesized at 20 °C at pH 5.0, 7.0 & 9.0 at time intervals of 24, 48 and 72 h.

and *P. aeruginosa* respectively as compared to control after 24 h of inoculation in disk diffusion assay (Fig. 7A). Similarly, in broth assay, maximum reduction was observed with spherical nanoparticles (2–5 nm) of smallest size showing 40, 51, 43, 53.9 and 55.8% of inhibition in *S. sonnei*, *E. coli*, *S. marcescens*, *S. aureus* and *P. aeruginosa* respectively in terms of log value of colony forming unit (CFU). Pentagonal and hexagonal nanoparticles demonstrated inhibition of 32, 41, 31, 42.84 and 42.80% of inhibition as compared to control (Fig. 7B). In both, plate and broth assay, maximum antagonistic effect of biosynthesized silver nanoparticles was observed with *S. aureus* and *P. aeruginosa* followed by *E. coli*.

Among the different shapes, when size of particles were similar, penta and hexagonal nanoparticles were most effective for antimicrobial activity, showing 15–18% more antagonistic effects on tested pathogens in comparison with spherical nanoparticles with 40–50 nm of size (Fig. 7A and B). Spherical nanoparticles of 2–5 nm were the most potent inhibitor of pathogen among all shape and size, showing 8–10% more efficacy as compared to penta and hexagons of 50–100 nm.

Nanoparticles are well known for their antimicrobial potential [5,44]. The properties of nanomaterials are strongly correlated with their morphology [7]. In this study, spherical nanoparticles of smallest size emerged as the best antimicrobial agent among the different shapes and sizes because of the high surface area to volume ratio. Agnihotri et al. [9] had demonstrated that antibacterial efficacy of silver nanoparticles gets enhanced significantly as the size of nanoparticles is reduced below 10 nm.

Triangular, penta and hexagonal also demonstrated good antibacterial potential though larger in size as compared to spherical one, because of sharp edges present in this particular morphology [7]. Wani et al. [45] also demonstrated the better antimicrobial properties of gold nanodiscs over gold polyhedral nanoparticles against *Candida* sp. This study generated an idea about equal role of shape and size in determining antimicrobial potential of biosynthesized nanoparticles.

3.4. Shape and size dependent synergistic antimicrobial activity of biosynthesized silver nanoparticles with antibiotics

To evaluate the synergistic effect of silver nanoparticles with different antibiotics, *S. marcescens* was selected due to its maximum resistance against penicillin and ampicillin. It also exhibited minimum zone of inhibition with other antibiotics and silver nanoparticles as compared to other pathogenic strains showing its high degree of tolerance. The zone of inhibition increased multifold when silver nanoparticles of different shape and size were tested concurrently with all selected antibiotics (Fig. 8 and S4). It was interesting to note that shape and size dependent synergistic effect of biogenic silver nanoparticles was observed only with those antibiotics against which pathogen has acquired resistance i.e. ampicillin and penicillin. Silver nanoparticles exhibited synergistic antimicrobial potential with

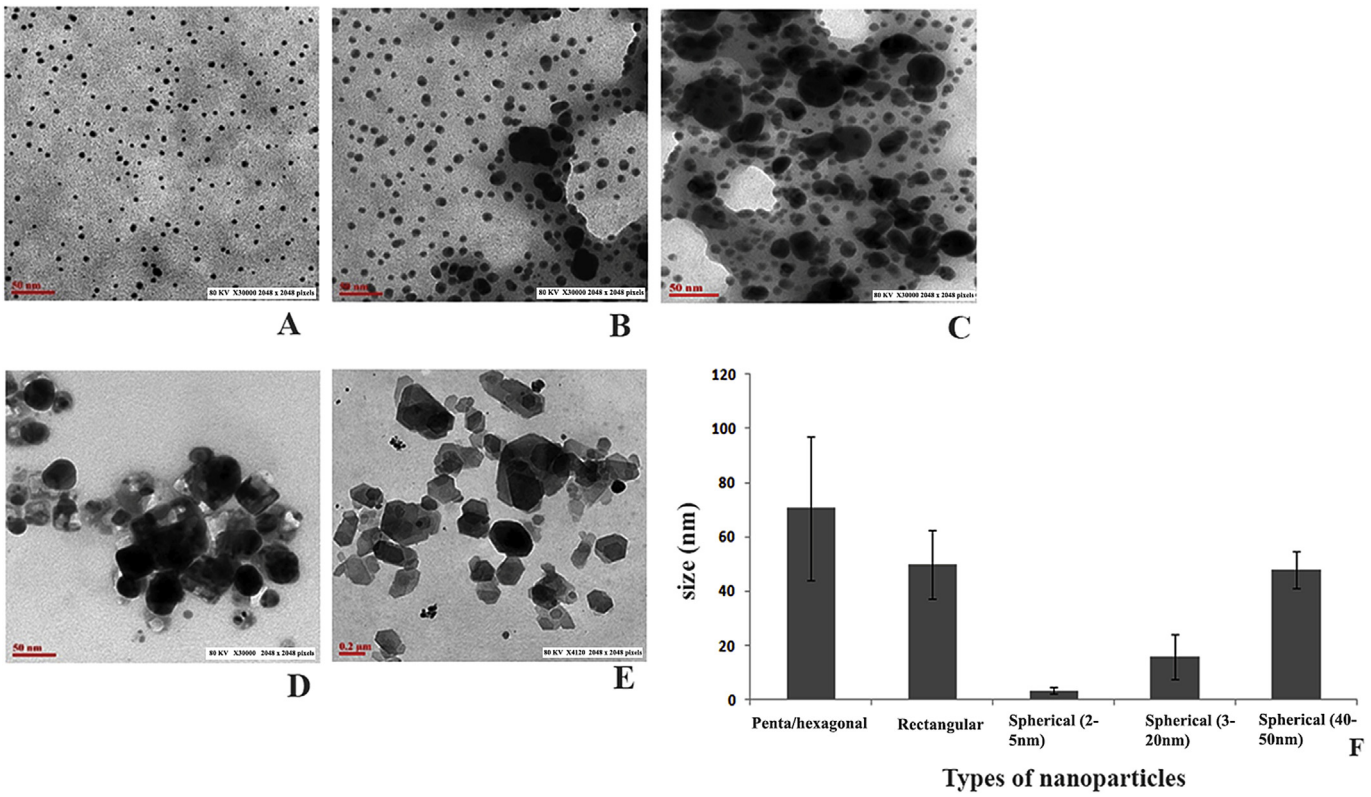

Fig. 6. TEM micrograph of biosynthesized silver nanoparticles of various shape and size (A) Penta and hexagonal (50–100 nm) (B) Rectangular (C) Spherical (2–5 nm) (D) Spherical (3–20 nm) (E) Spherical (40–50 nm) (F) particle size distribution during TEM size measurement.

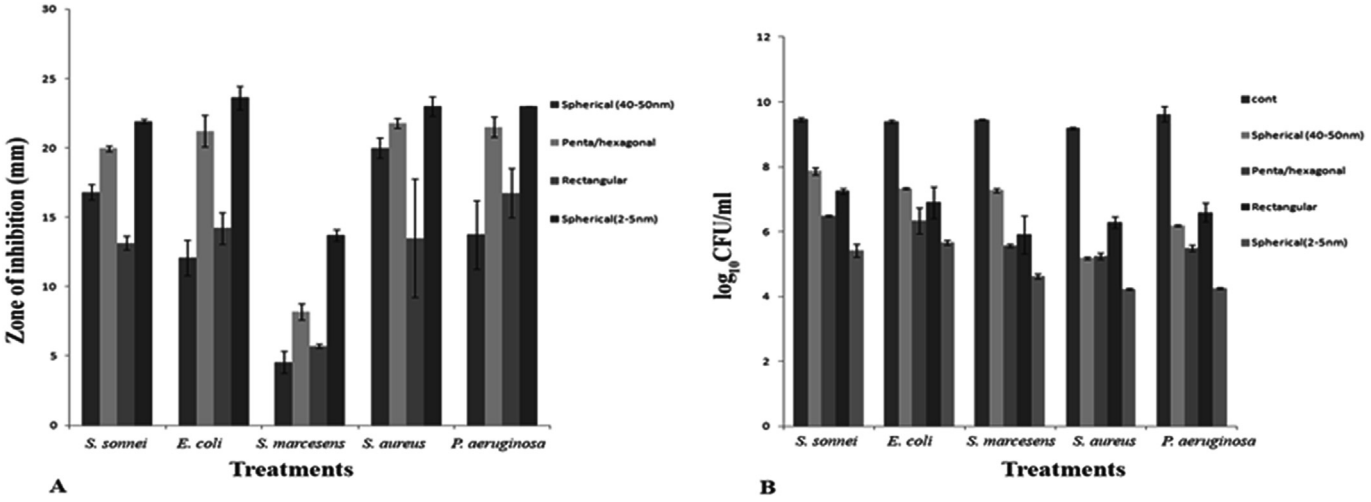

Fig. 7. Shape and size dependent antimicrobial activity of biogenic silver nanoparticles against *S. sonnei*, *E. coli and S. marcescens* (A) Zone of inhibition (mean) in plate assay (B) $\log_{10}$ CFU/ml population of human pathogens in broth assay.

streptomycin, kanamycin and tetracyclin but it was not dependent upon the morphology and dimension of silver nanoparticles (Fig. S4). The smallest biosynthesized nanoparticle (2–5 nm) proved as the strongest blueprint to enhance the efficacy of ampicillin and penicillin against multidrug resistant pathogens. Penta, hexagonal and rectangular nanoparticles of 50–100 nm also demonstrated significant increase in zone of inhibition of 45 and 40% respectively with ampicillin and penicillin as compared to the spherical nanoparticles with 40–50 nm of dimension (Fig. 8B).

All kind of shape and size of biologically synthesized silver nanoparticles demonstrated similar synergistic increase in zone of inhibition with streptomycin, kanamycin and tetracycline as compared to respective antibiotic control (Fig. 7A). The most pronounced synergistic effect was observed with tetracyclin, followed by ampicillin.

Synergistic effects of silver nanoparticles with antibiotics is also reported in literature but the shape and size dependent activity of silver nanoparticles with antibiotics still remains unknown. This study provides an insight into the shape and size dependent synergistic antimicrobial potential of biogenic silver nanoparticles

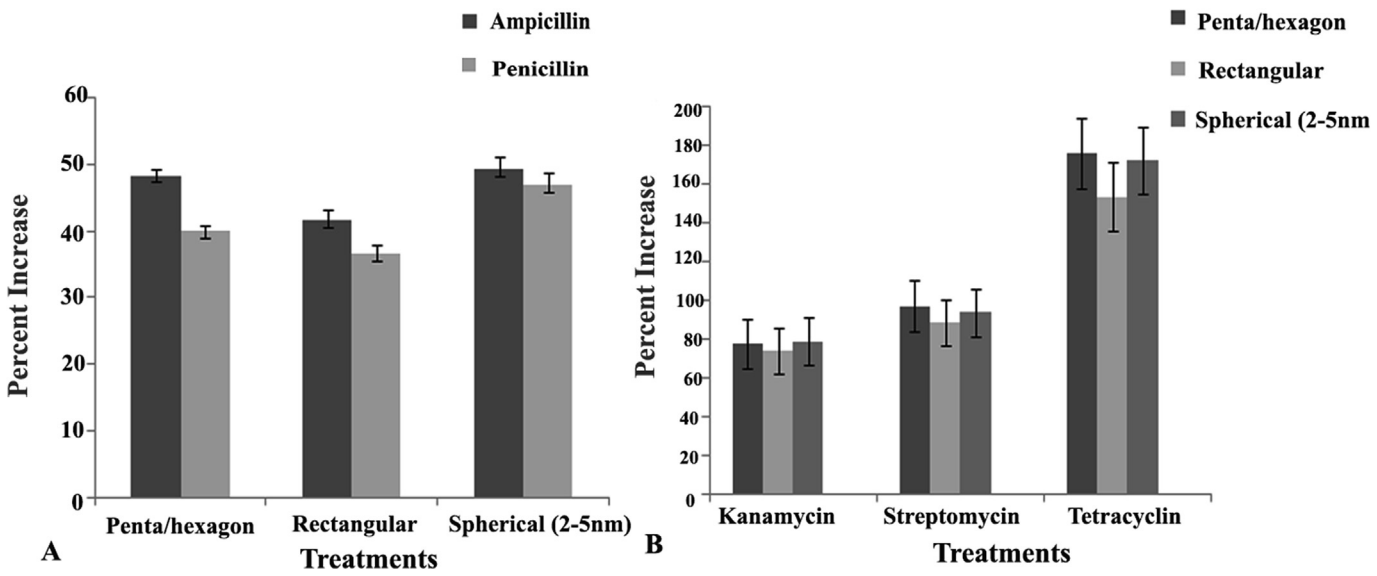

Fig. 8. Synergistic effect of biogenic silver nanoparticles of different shape and size with antibiotics against *S. marcescens* (A) Percent increase in antimicrobial activity of different shape and size of silver nanoparticles with antibiotics in comparison with spherical nanoparticles of 40–50 nm (B) Percent increase in antimicrobial activity of different shape and size of silver nanoparticles with antibiotics in comparison with their respective antibiotic alone.

with different antibiotics. In accordance with the previous results, nanosphere of 2–5 nm and pentagonal and hexagonal nanoparticles demonstrated the best antibacterial potential with ampicillin and penicillin. The pathogen had acquired resistance against ampicillin and penicillin, but when silver nanoparticles were applied simultaneously with antibiotics, it yielded a clear zone of inhibition, which was dependent upon the size and morphology of the nanoparticles (Fig. S4). With ampicillin, penta and hexagonal particles of 50–100 nm were efficient as spherical nanoparticles of 2–5 nm. With the sharp edges and small size, penta and hexagonal particles can provide more synergistic effects towards MDR pathogens. With the antibiotics to which the pathogen was susceptible, there was a synergistic increase in zone of inhibition when both antibiotics and silver nanoparticles were applied simultaneously; however the increase was not dependent upon the morphology and dimension of biogenic particles.

Pathogens acquiring multidrug resistance possess a threat and has become a serious health problem [46]. To fight multidrug resistance, silver nanoparticles have proved their candidature as an absolute formulation additive for antibiotics [7,47].

4. Conclusions

A simple, green and economical approach to modulate shapes and sizes of silver nanoparticles was investigated. Spherical (2–5 nm), rectangular (40–65 nm) and penta/hexagonal (50–100 nm) silver nanoparticles were obtained by varying pH, reaction time and temperature of the reaction mixture. Smallest spherical (2–5 nm) nanoparticles were obtained at 30 °C, pH 7.0 after 24 h of incubation. This study concluded that mutually dependent exclusive balance of physical parameters is responsible for bioengineering of nanoparticles. Maximum antibacterial activity was observed with spherical nanoparticles (2–5 nm) showing 40, 51, 43, 53.9 and 55.8% against *S. sonnei*, *E. coli*, *S. marcescens*, *S. aureus* and *P. aeruginosa* respectively, where as pentagonal and hexagonal nanoparticles (50–100 nm) demonstrated 32, 41, 31, 42.84 and 42.80% of inhibition as compared to control at the same concentration of nanoparticles. Synergistic effects of biogenic silver nanoparticles with antibiotics against which bacteria have acquired resistance were observed in a morphology dependent manner. Synchronization of the most potent silver nanoparticles along with antibiotics could be a very effective formulation additive to the antibiotics in inhibiting the growth of multidrug resistant pathogens. Present findings have immense potential in biomedical application for overcoming the problem of MDR bacteria.

Acknowledgements

We thank CSIR- Indian Institute of Toxicology Research and Dr L. K. S. Chauhan for guiding us in use of TEM. This study was partially funded by network project of Council of Scientific and Industrial Research (BSC0117) “Plant Microbe Soil Interactions BSC 117”. The authors thank CSIR for awarding Senior Research Fellowship (SRF) to Madhuree Kumari.

Appendix A. Supplementary data

Supplementary data related to this article can be found at http://dx.doi.org/10.1016/j.micpath.2016.11.012.

References

[1] M. Eugenio, N. Müller, S. Frasés, R. Almeida-Paes, T.R.L. Lima, L. Lemgruber, M. Farina, W. de Souza, C. Sant'Anna, Yeast-derived biosynthesis of silver/silver chloride nanoparticles and their antiproliferative activity against bacteria, RSC Adv. 6 (2016) 9893.
[2] S. Shanthi, B.D. Jayaseelan, P. Velusamy, S. Vijayakuma, C.T. Chih, B. Vaseeharan, Biosynthesis of silver nanoparticles using a probiotic *Bacillus licheniformis* Dahb1 and their antibiofilm activity and toxicity effects in *Ceriodaphnia cornuta*, Microb. Pathog. 93 (2016) 70.
[3] M. Latha, M. Sumathi, R. Manikandan, A. Arumugam, N.M. Prabhu, Biocatalytic and bactericidal interaction visualization of green synthesized silver nanoparticles using *Hemidesmus indicus*, Microb. Pathog. 82 (2015) 43.
[4] M. Latha, M. Priyanka, P. Rajasekar, R. Manikandan, N.M. Prabhu, Biocompatibility and antibacterial activity of the Adathoda vasica Linn extract mediated silver nanoparticles, Microb. Pathog. 93 (2016) 88.
[5] O. Choi, Z. Hu, Size dependent and reactive oxygen species related nanosilver toxicity to nitrifying bacteria, Environ. Sci. Technol. 42 (2008) 4583.
[6] S. Pal, Y.L. Tak, J.Y. Song, Does the antibacterial activity of silver nanoparticles depend on the shape of the nanoparticle? A study of the gram-negative bacterium *Escherichia coli*, Appl. Environ. Microbiol. 73 (2007) 1712.
[7] P.V. Dong, C.H. Ha, L.T. Binh, J. Kasbohm, Chemical synthesis and antibacterial activity of novel-shaped silver nanoparticles, Int. Nano Lett. 2 (2012) 9.

[8] S. Agnihotri, S. Mukherji, S. Mukherji, Size-controlled silver nanoparticles synthesized over the range 5–100 nm using the same protocol and their antibacterial efficacy, RSC Adv. 4 (2014) 3974.
[9] S.K. Das, A.R. Das, A.K. Guha, Microbial synthesis of multishaped gold nanostructures, Small 6 (2010) 1012.
[10] T.M. Tolaymat, A.M. El Badawy, A. Genaidy, K.G. Scheckel, T.P. Luxton, M. Suidan, An evidence-based environmental perspective of manufactured silver nanoparticle in syntheses and applications: a systematic review and critical appraisal of peer-reviewed scientific papers, Sci. Total Environ. 408 (2010) 999.
[11] A. Panáček, R. Prucek, J. Hrbáč, T. Nevečná, J. Šteffková, R. Zbořil, L. Kvítek, Polyacrylate-assisted size control of silver nanoparticles and their catalytic activity, Chem. Mater 26 (2014) 1332.
[12] N.I. Hulkoti, T.C. Taranath, Biosynthesis of nanoparticles using microbes- a review, Colloids Surf. B Biointerfaces 121 (2014) 474.
[13] N. Kaushik, M. Thakkar, S. Snehit, M.S. Mhatre, Y. Rasesh, M.S. Parikh, Biological synthesis of metallic nanoparticles, Nanomed Nanotechnol. Biol. Med. 6 (2010) 257.
[14] J.Y. Song, B.S. Kim, Rapid biological synthesis of silver nanoparticles using plant leaf extracts, Bioprocess Biosyst. Eng. 32 (2009) 79.
[15] G. Wang, H. Mitomo, Y. Matsuo, K. Niikura, M. Maeda, K. Ijiro, DNA-modulated photo-transformation of AgCl to silver nanoparticles: visiting the formation mechanism, Colloid Interface Sci 452 (2015) 224.
[16] S.K. Das, M.R. Khan, T. Parandhaman, F. Laffir, A.K. Guha, G. Sekarana, A.B. Mandal, Nano-silica fabricated with silver nanoparticles: antifouling adsorbent for efficient dye removal, effective water disinfection and biofouling control, Nanoscale 5 (2013) 5549.
[17] A. Mishra, M. Kumari, S. Pandey, V. Chaudhry, K.C. Gupta, C.S. Nautiyal, Biocatalytic and antimicrobial activities of gold nanoparticles synthesized by *Trichoderma* sp, Bioresour. Technol. 166 (2014) 235.
[18] M. Kumari, A. Mishra, S. Pandey, S.P. Singh, V. Chaudhry, M.K.R. Mudiam, S. Shukla, P. Kakkar, C.S. Nautiyal, Physico-chemical condition optimization during biosynthesis lead to development of improved and catalytically efficient gold nano particles, Sci. Rep. 6 (2016) 27575.
[19] L. Tang, K. Huynh, M.L. Fleming, M. Larronde-Larretche, K.L. Chen, Imparting antimicrobial and anti-adhesive properties to polysulfone membranes through modification with silver nanoparticles and polyelectrolyte multilayers, Colloid Interface Sci 451 (2015) 125.
[20] G.C. Kumar, Y. Poornachandra, Biodirected synthesis of Miconazole-conjugated bacterial silver nanoparticles and their application as antifungal agents and drug delivery vehicles, Colloids Surf. B Biointerfaces 125 (2015) 110.
[21] M.S. Ud-Din, S.U.L. Wahid, H.A. Latif, M. Shahnaij, M. Akter, et al., Changing trends in the prevalence of *Shigella* species: emergence of multi-drug resistant *Shigella sonnei* Biotype g in Bangladesh, PLoS One 8 (2013) e82601.
[22] G.C. Perron, S. Kryazhimskiy, D.P. Rice, A. Buckling, Multidrug therapy and evolution of antibiotic resistance: when order matters, Appl. Environ. Microbiol. 78 (2012) 6137.
[23] T. Bollenbach, Antimicrobial interactions: mechanisms and implications for drug discovery and resistance evolution, Curr. Opin. Microbiol. 27 (2015) 1.
[24] M.V. Sujitha, S. Kannan, Green synthesis of gold nanoparticles using Citrus fruits (*Citrus limon*, *Citrus reticulata* and *Citrus sinensis*) aqueous extract and its characterization, Spectrochim. Acta A Mol. Biomol. Spectrosc. 102 (2013) 15.
[25] P.K. Singh, P. Tripathi, S. Dwivedi, S. Awasthi, M. Shri, D. Chakrabarty, R.D. Tripathi, Fly-ash augmented soil enhances heavy metal accumulation and phytotoxicity in rice (Oryza sativa L.); A concern for fly-ash amendments in agriculture sector, Plant Growth Regul. 78 (2016) 21.
[26] M.A. Munger, P. Radwanski, G.C. Hadlock, G. Stoddard, A. Shaaban, J. Falconer, D.W. Grainger, C.E. Deering-Rice, *In vivo* human time-exposure study of orally dosed commercial silver nanoparticles, Nanomed Nanotechnol. BiolMed 10 (2014) 1.
[27] S. Bhattacharjee, DLS and zeta potential – what they are and what they are not? J. Cont. Release 235 (2016) 337.
[28] K. Vahabi, G.A. Mansoori, S. Karimi, Biosynthesis of silver nanoparticles by fungus *Trichoderma reesei* (a route for large-scale production of AgNPs), Insciences J. 1 (2011) 65.
[29] S.A. Kustrin, D.W. Morton, A. Pauzi, M. Yusof, The use of fourier transform infrared (FTIR) spectroscopy and artificial neural networks (ANNs) to assess wine quality, Mod. Chem. Appl. 1 (2013) 4.
[30] S.S. Shankar, A. Rai, A. Ahmad, S. Sastry, Rapid synthesis of Au, Ag, and bimetallic Au core-Ag shell nanoparticles using Neem (*Azadirachta indica*) leaf broth, J. Colloid Interf. Sci. 275 (2004) 496.
[31] D. Starnes, A. Jain, S.V. Sahi, In planta engineering of gold nanoparticles of desirable geometries by modulating growth conditions: an environment-friendly approach, Environ. Sci. Technol. 44 (2010) 7110.
[32] S. Iravani, Green synthesis of metal nanoparticles using plants, Green Chem. 13 (2011) 2638.
[33] R. Jin, Y.W. Cao, C.A. Mirkin, K.A. Kelly, G.C. Schatz, S.G. Zheng, Photoinduced conversion of silver nanospheres to nanoprisms, Science 294 (2001) 1901.
[34] M.R. Langille, M.L. Personick, L. Zhang, C.A. Mirkin, Defining rules for the shape evolution of gold nanoparticles, J. Am. Chem. Soc. 134 (2012) 14542.
[35] J. Zhu, S. Liu, O. Palchik, Y. Koltypin, A. Gedanken, Shape-controlled synthesis of silver nanoparticles by pulse sonoelectrochemical methods, Langmuir 16 (2000) 639.
[36] S.K. Balavandy, K. Shameli, D.R.B.A. Biak, Z.Z. Abidin, Stirring time effect of silver nanoparticles prepared in glutathione mediated by green method, Chem. Cent. J. 8 (2014) 11.
[37] S. Hussain, R. Akrema, Z. Khan, Extracellular biosynthesis of silver nanoparticles: effects of shape-directing cetyltrimethylammonium bromide, pH, sunlight and additives, Bioprocess Biosyst. Eng. 37 (2014) 953.
[38] X.C. Jiang, W.M. Chen, C.Y. Chen, X.Y. Xiong, A.B. Yu, Role of temperature in the growth of silver nanoparticles through a synergetic reduction approach, Nanoscale. Res. Lett. 6 (2011) 32.
[39] G.P. Lee, Y. Shi, E. Lavoie, P. Daeneke, P. Reineck, U.B. Cappel, D.M. Huang, U. Bach, Light-driven transformation processes of anisotropic silver nanoparticles, ACS Nano 7 (2014) 911.
[40] M.A. Mahmoud, D. O'Neil, M.A. El-Sayed, High-frequency mechanical stirring initiates anisotropic growth of seeds requisite for synthesis of asymmetric metallic nanoparticles like silver nanorods, Nano Lett. 14 (2014) 743.
[41] B. Tang, L. Sun, J. Li, M. Zhang, X. Wang, Sunlight-driven synthesis of anisotropic silver nanoparticles, Chem. Eng. J. 260 (2015) 99.
[42] A.B. Kajani, A.K. Bordbar, S.Z.H. Esfahani, A.R. Khosropour, A. Razmjou, Green synthesis of anisotropic silver nanoparticles with potent anticancer activity using *Taxus baccata* extract, RSC Adv. 4 (2014) 61394.
[43] X. Xia, J. Zeng, Q. Zhang, Q.H. Moran, Y. Xia, Recent developments in shape-controlled synthesis of silver nanocrystals, J. Phys. Chem. C 116 (2012) 21647.
[44] A. Taglietti, C.R. Arciola, A. D'Agostino, G. Dacarro, L. Montanaro, D. Campoccia, et al., Antibacterial activity of glutathione-coated silver nanoparticles against Gram positive and Gram negative bacteria, Biomat 35 (2014) 1779.
[45] I.A. Wani, T. Ahmad, N. Manzoor, Size and shape dependant antifungal activity of gold nanoparticles: a case study of Candida, Colloids Surf. B Biointerfaces 101 (2013) 162.
[46] M. Bassetti, E. Righi, Multidrug-resistant Bacteria: what Is the Threat?, Hematology Am Soc Hematol Educ Program 2013, 2013, p. 428.
[47] M.A. Ansari, H.M. Khan, A.A. Khan, S.S. Cameotra, Q. Saquiband, J. Musarrat, Gum arabic capped-silver nanoparticles inhibit biofilm formation by multidrug resistant strains of *Pseudomonas aeruginosa*, J. Basic Microbiol. 54 (2014) 1.